XYZ production at the EIC

Derek Glazier
University of Glasgow

XYZ

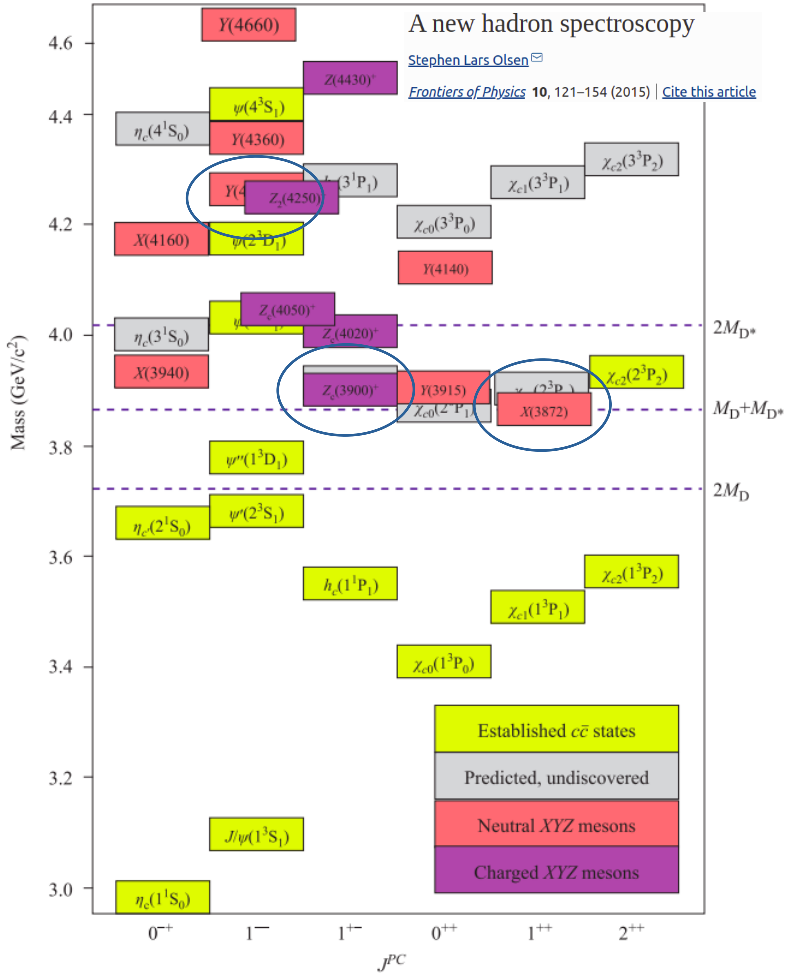

Quarkonium models
 => allowed states of a heavy $Q\bar{Q}$ system
Meson decays to final state
with a Q and a $\bar{Q}$,
but not matching the $Q\bar{Q}$ spectrum,
=> necessarily exotic.

→ XYZ charmoniumlike mesons

$$e^+e^- \to \pi^+\pi^- J/\psi \ (4260 \text{ MeV})$$

e.g. $Z_c^{+-}(3900)$
=> requires
 4 quarks

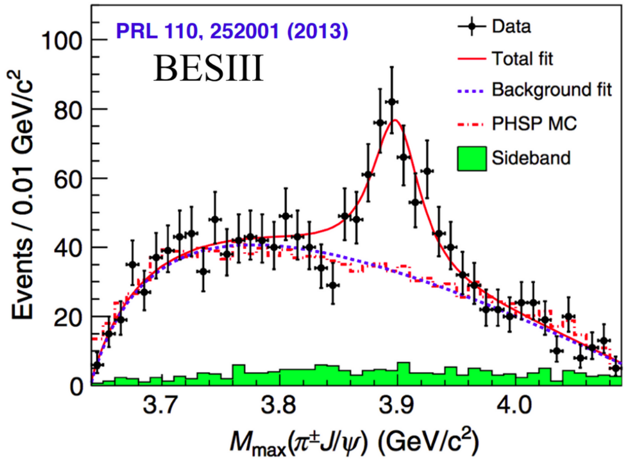

Exclusive Photoproduction (Quasi-real)

Observation of XYZ states in photoproduction
- independent confirmation

Different production mechanism, different kinematics

Measurement of polarisation observables and photocouplings
- insights into production mechanisms and internal structure

XYZ spectroscopy at electron-hadron facilities: Exclusive processes

M. Albaladejo, A. N. Hiller Blin, A. Pilloni, D. Winney, C. Fernández-Ramírez, V. Mathieu, and A. Szczepaniak
(Joint Physics Analysis Center)
Phys. Rev. D **102**, 114010 – Published 7 December 2020

- qualitative behaviour and order of magnitude estimates

X(3872) at COMPASS

Physics Letters B
Volume 783, 10 August 2018, Pages 334-340

Search for muoproduction of $X(3872)$ at COMPASS and indication of a new state $\widetilde{X}(3872)$

Similar production mechanism

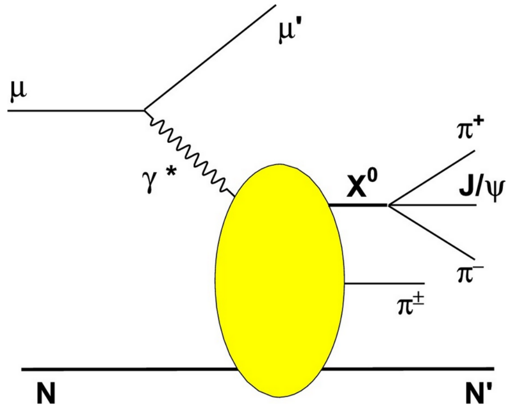

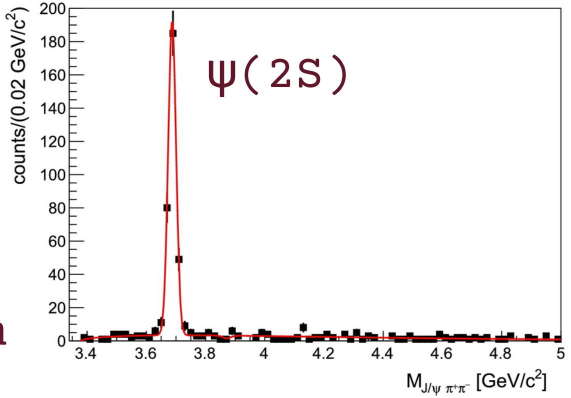

Little signal in direct J/ψππ

But X like peak
Seen when produced
With extra pion

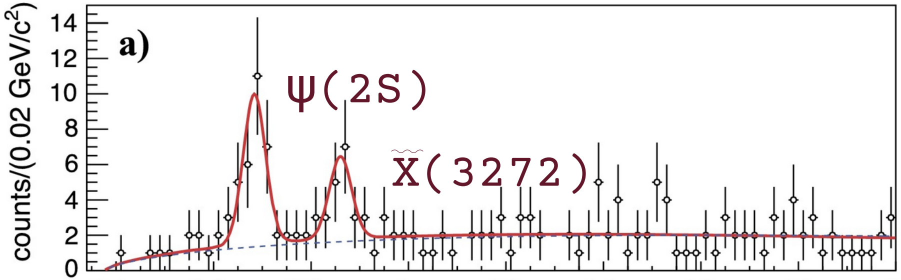

Suggest a 1+- state instead of 1++ …

Event Generator (Pictorial)

Factorise 2 photon vertices

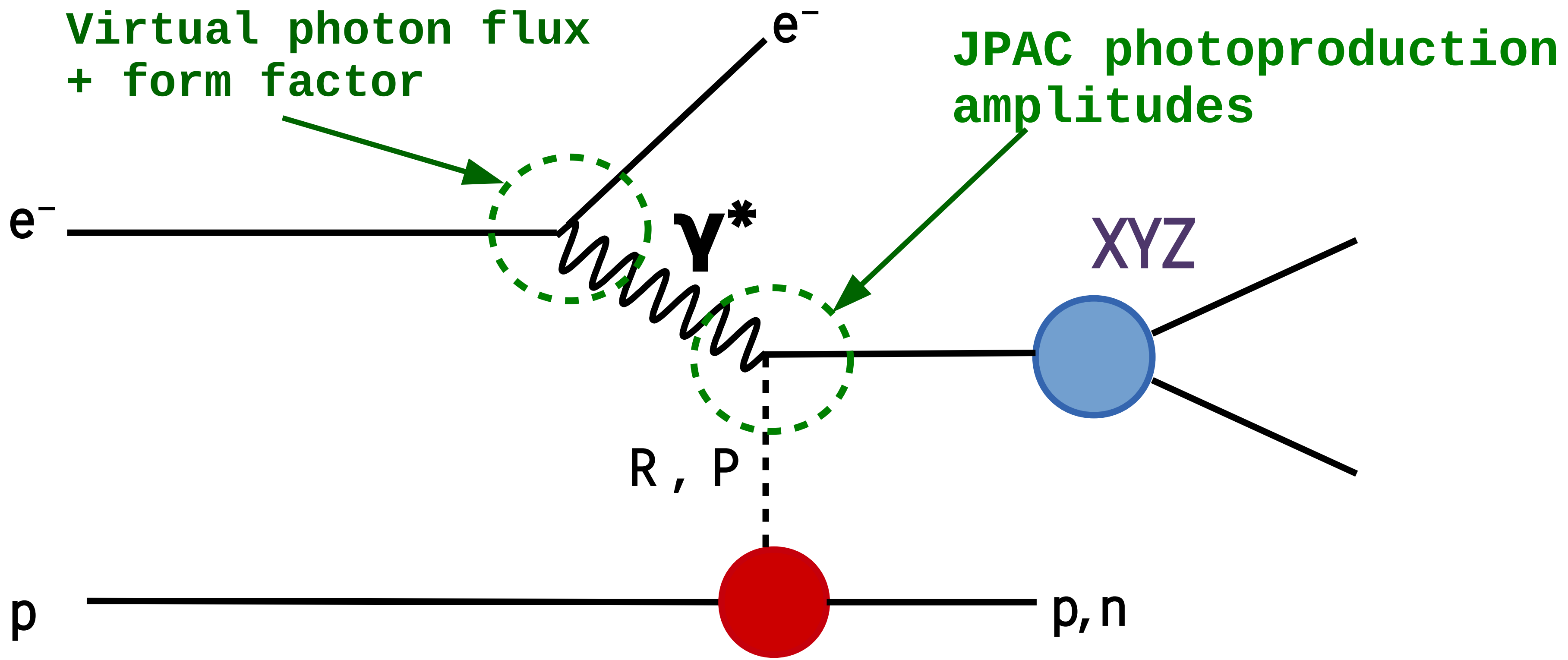

Event Generator (Formal)

$$\frac{d^4\sigma}{ds\,dQ^2\,d\phi\,dt} = \frac{d^2\sigma_{e,\gamma*e'}}{dsdQ^2}\frac{d^2\sigma_{\gamma*+p\rightarrow V+p}(s,Q^2)}{d\phi\,dt}$$

→ Integrate for event rate

$$Q^2 = 2\,E\,M\,x\,y$$

$$W^2 = M^2 + 2\,E\,M\,y - Q^2$$

$$\frac{d^2\sigma_{e,\gamma*e'}}{dsdQ^2} = \frac{\alpha}{2\pi}\cdot\frac{K.L}{E}\cdot\frac{1}{Q^2}\cdot\frac{1}{(s-M^2+Q^2)}$$

$$L = \frac{1+(1-y)^2}{y} - \frac{2m_e^2\,y}{Q^2}$$

$$K = \frac{W^2-M^2}{2M} = \nu(1-x) = Ey(1-x) = \nu - \frac{Q^2}{2M}$$

$$\frac{d^2\sigma_{\gamma*+p}}{d\phi\,dt} = \frac{d\sigma^T(Q^2,s)}{d\phi\,dt} + (\epsilon+\delta)\frac{d\sigma^L(Q^2,s)}{d\phi\,dt}$$

$$\frac{d^2\sigma^T(Q^2,s)}{d\phi\,dt} = \frac{d^2\sigma_{\gamma+p\rightarrow V+p}}{d\phi\,dt}F(Q^2)$$

$$\frac{d^2\sigma^L(Q^2,s)}{d\phi\,dt} = 0$$

$$\frac{d^2\sigma_{\gamma+p\rightarrow V+p}}{d\phi\,dt} = \frac{1}{128\pi^2 s}\frac{1}{|\mathbf{p}_{\gamma*cm}|^2}|M(s,t)|^2$$

→ $|M(s,t)|^2$ JPAC Photoproduction Amplitudes

EIC-smear benchmarks

Representative Luminosities For various EIC settings

L ($10^{33} cm^{-2} s^{-1}$)	5-41 W_{max}=29	5-100 W_{max}=45	10-100 W_{max}=64	18-275 W_{max}=100
Low CM Optimised	1. ?	10 ?	10 ?	0
High CM Optimised	0.44	3.68	4.48	1.54

Benchmarks performed for 1fb^{-1} of integrated charge(11.6days@$10^{33} cm^{-2} s^{-1}$)

Use interpolated high and low Jpac amplitudes

Use approximate branching ratios for XYZ (from JPAC paper)

Z(3900)

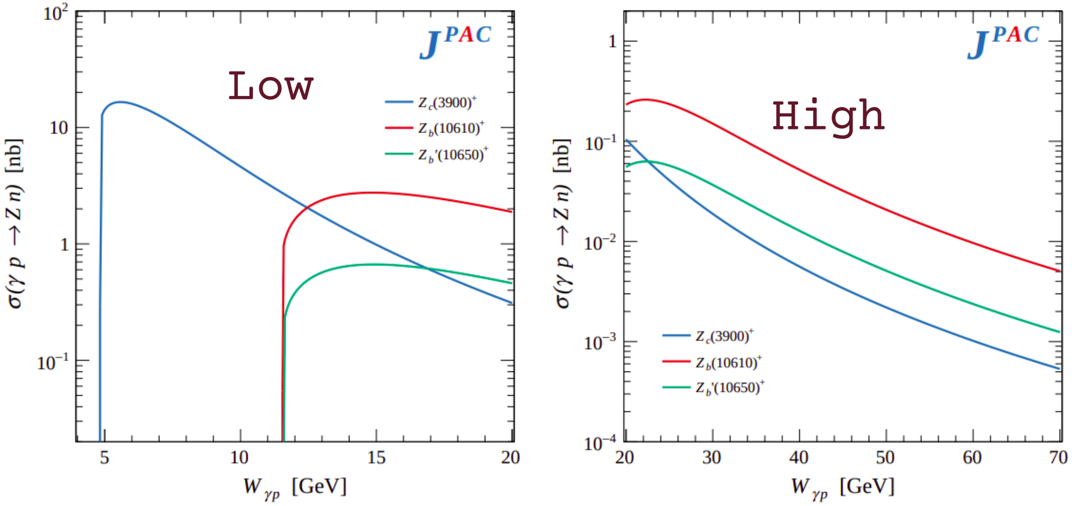

FIG. 2. Integrated cross sections for the three Z states considered. Left panel: predictions for fixed-spin exchange, which we expect to be valid up to approximately 10 GeV above each threshold. Right panel: predictions for Regge exchange, valid at high energies.

Larger at Low W,
Small at High W

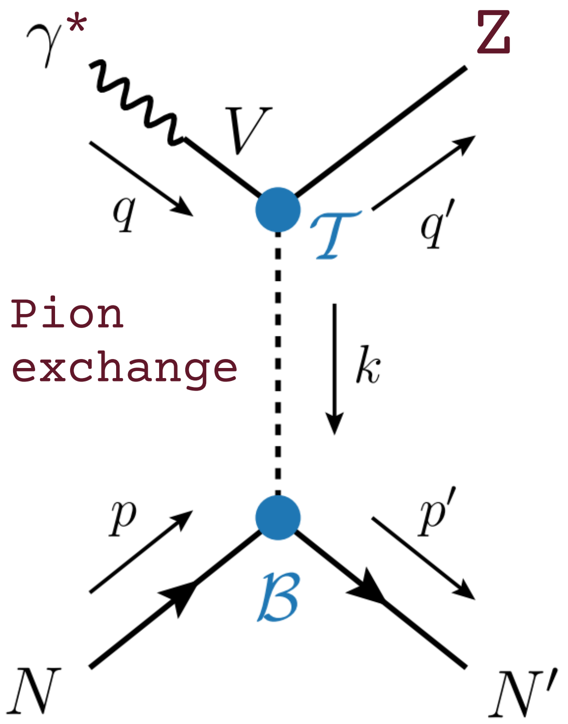

Z(3900)

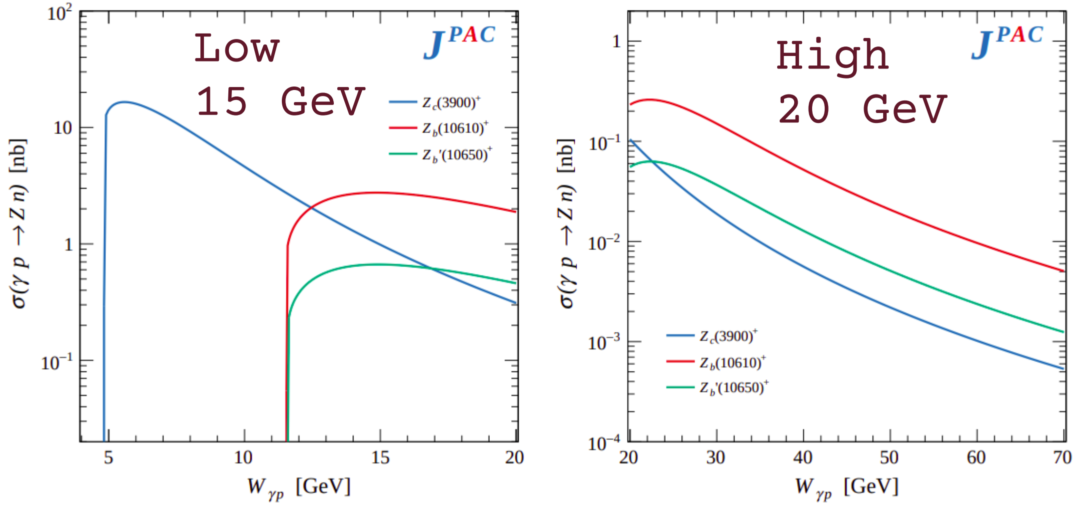

FIG. 2. Integrated cross sections for the three Z states considered. Left panel: predictions for fixed-spin exchange, which we expect to be valid up to approximately 10 GeV above each threshold. Right panel: predictions for Regge exchange, valid at high energies.

$e^- + p \to e^{-\prime} + Z(3900) + n$
$Z \to J/\psi\ \pi^+$ (10%)
$J/\psi \to e^+e^-$ (6%)

For 1 fb^{-1} ~11 days @ $10^{33}cm^{-2}s^{-1}$

Use eic-smear with
MATRIXDETECTOR_0_2_B1_5T

Ngen → number generated
NZ → number detected
NZ e → NZ with detected e-

	Ngen	NZ	NZ e
5-41	2.6k	2.4k	150
5-100	3.0k	2.0k	160
10-100	3.3k	2.1k	50
18-275	2.5k	0.7k	8

Z 5-100 MATRIXDETECTOR_0_2_B1_5T

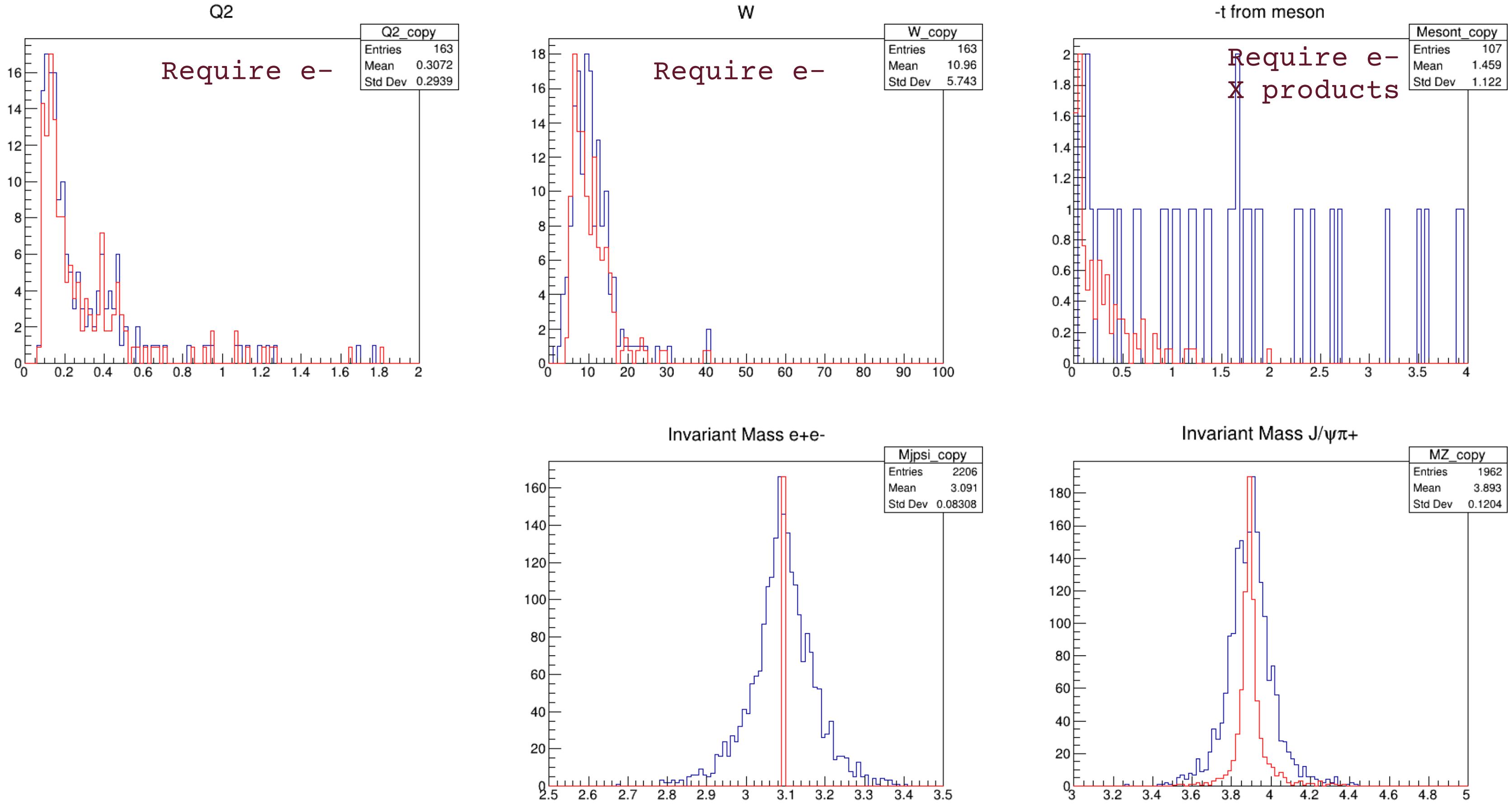

Generated
EIC-Smeared

Normalised to
Same max value

Y(4260)

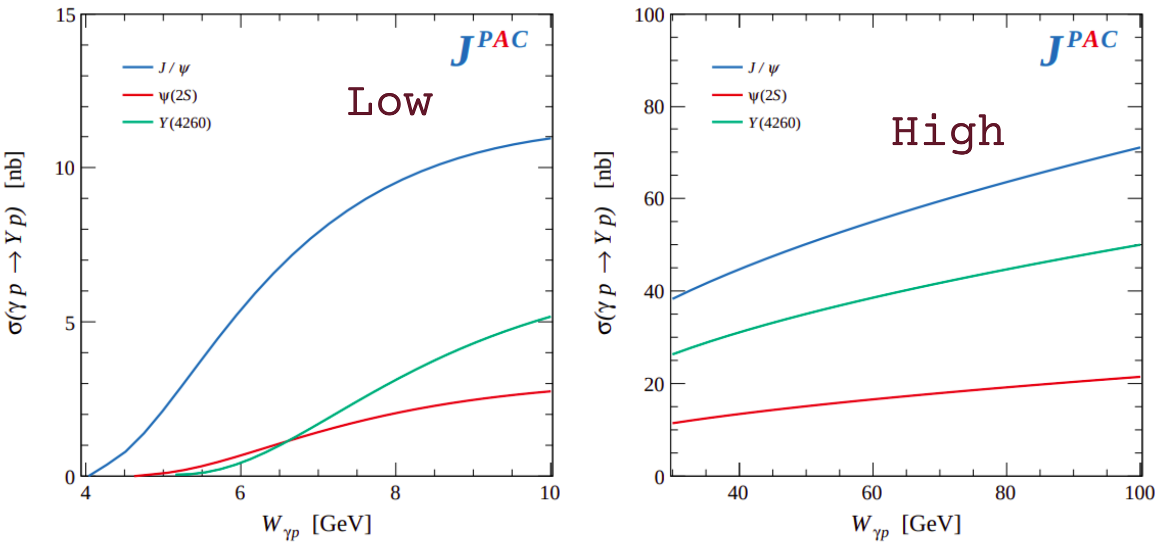

FIG. 7. Cross sections for $Y(4260)$ photoproduction compared to the J/ψ and $\psi(2S)$ at low (left) and high (right) energies.

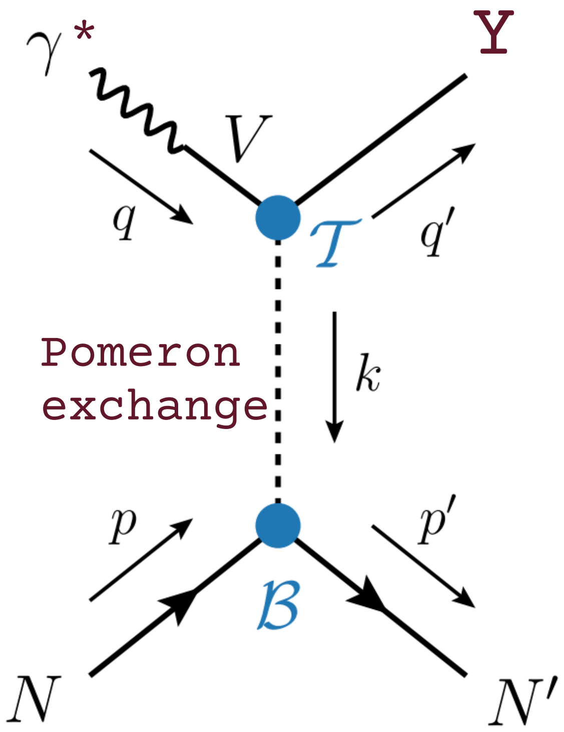

Increases with W

Y(4260)

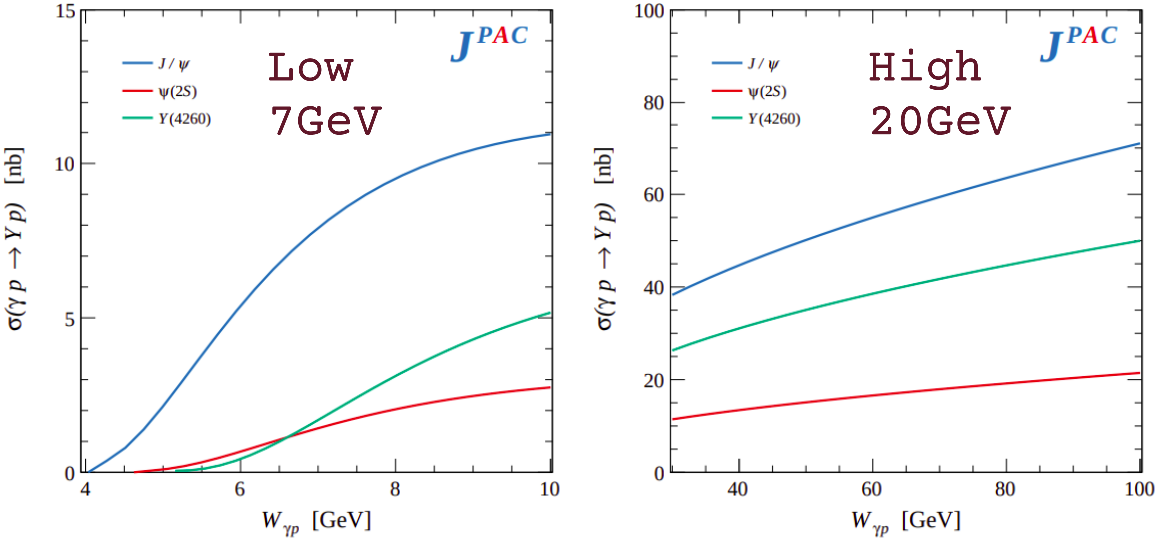

FIG. 7. Cross sections for $Y(4260)$ photoproduction compared to the J/ψ and $\psi(2S)$ at low (left) and high (right) energies.

$e^- + p \rightarrow e^{-\prime} + Y(4260) + p$

$Y \rightarrow J/\psi\ \pi^+\pi^+$ (1%)

$J/\psi \rightarrow e^+e^-$ (6%)

For 1 fb^{-1} ~11 days @ 10^{33}cm-2s-1

Use eic-smear with
MATRIXDETECTOR_0_2_B1_5T

Ngen → number generated
NY → number detected
NY+e' → NY with detected e-

	Ngen	NY	NY + e'
5-41	2.2k	900	180
5-100	2.2k	2.2k	375
10-100	3.7k	3.6k	290
18-275	8.7k	7.9k	270

Y 5-100 MATRIXDETECTOR_0_2_B1_5T

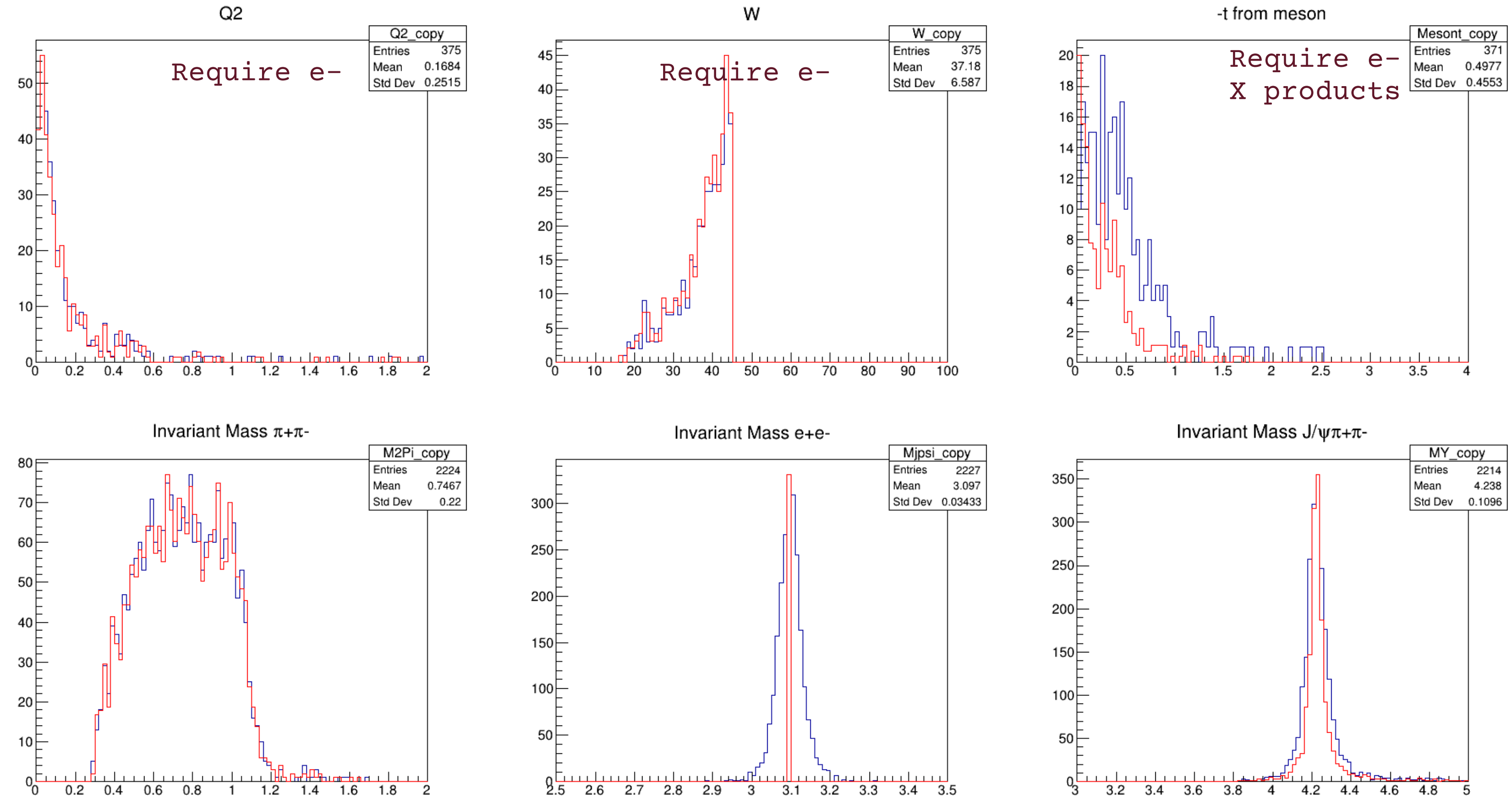

Generated
EIC-Smeared

Normalised to Same max value

Υ Decay product distributions

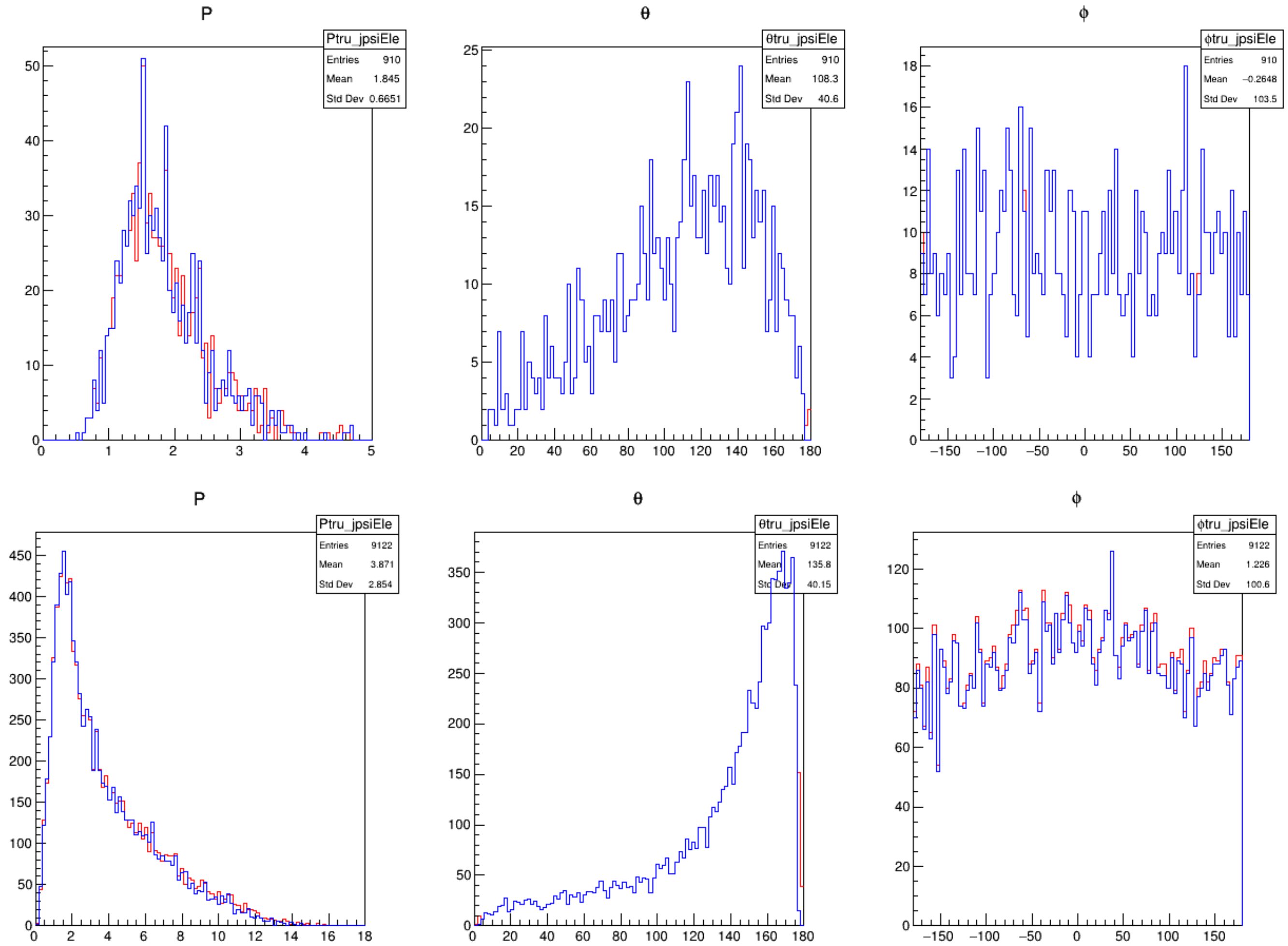

Jpsi e-

Generated

EIC-Smeared

5-41

At large W

Products → e-

18-275

X(3872)

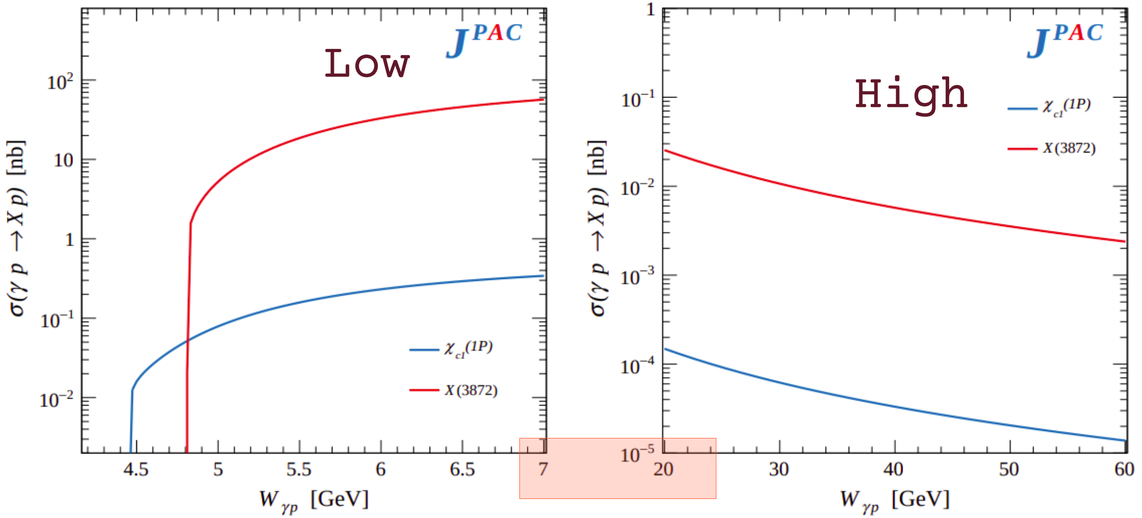

FIG. 3. Integrated cross sections for the axial $\chi_{c1}(1P)$ and $X(3872)$. Left panel: predictions for fixed-spin exchange, valid at low energies. Right panel: predictions for Regge exchange, valid at high energies.

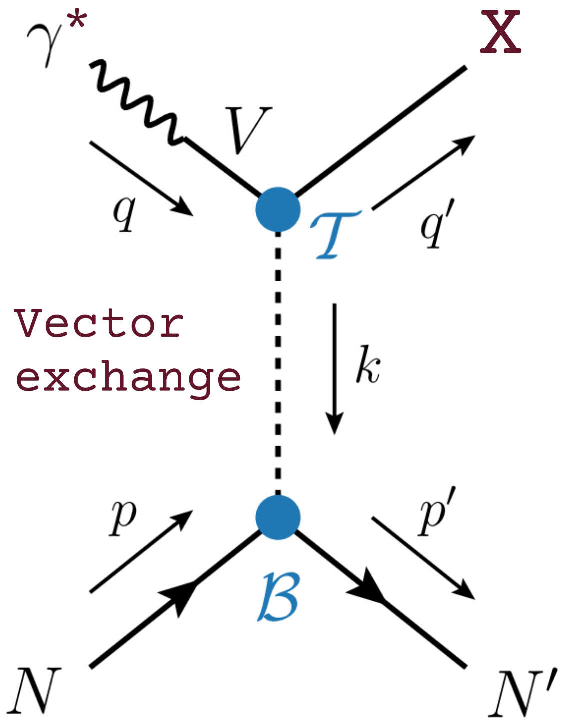

Larger model uncertainty

X(3872)

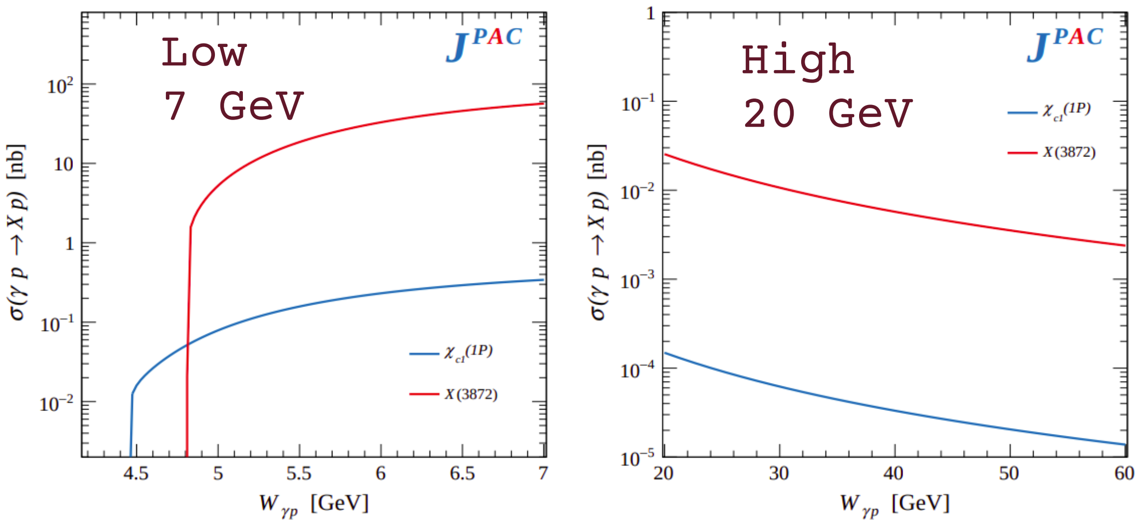

FIG. 3. Integrated cross sections for the axial $\chi_{c1}(1P)$ and $X(3872)$. Left panel: predictions for fixed-spin exchange, valid at low energies. Right panel: predictions for Regge exchange, valid at high energies.

$e^- + p \to e^{-'} + X(3872) + p$

$X \to J/\psi\ \pi^+\pi^+$ (5%)

$J/\psi \to e^+e^-$ (6%)

For 1 fb^{-1} ~11 days @ 10^{33}cm-2s-1

Use eic-smear with
MATRIXDETECTOR_0_2_B1_5T

	Ngen	NX	NX + e’
5-41	10k	9k	650
5-100	11k	9k	660
10-100	13k	10k	170
18-275	10k	3.7k	25

X 5-100 MATRIXDETECTOR_0_2_B1_5T 0mrad

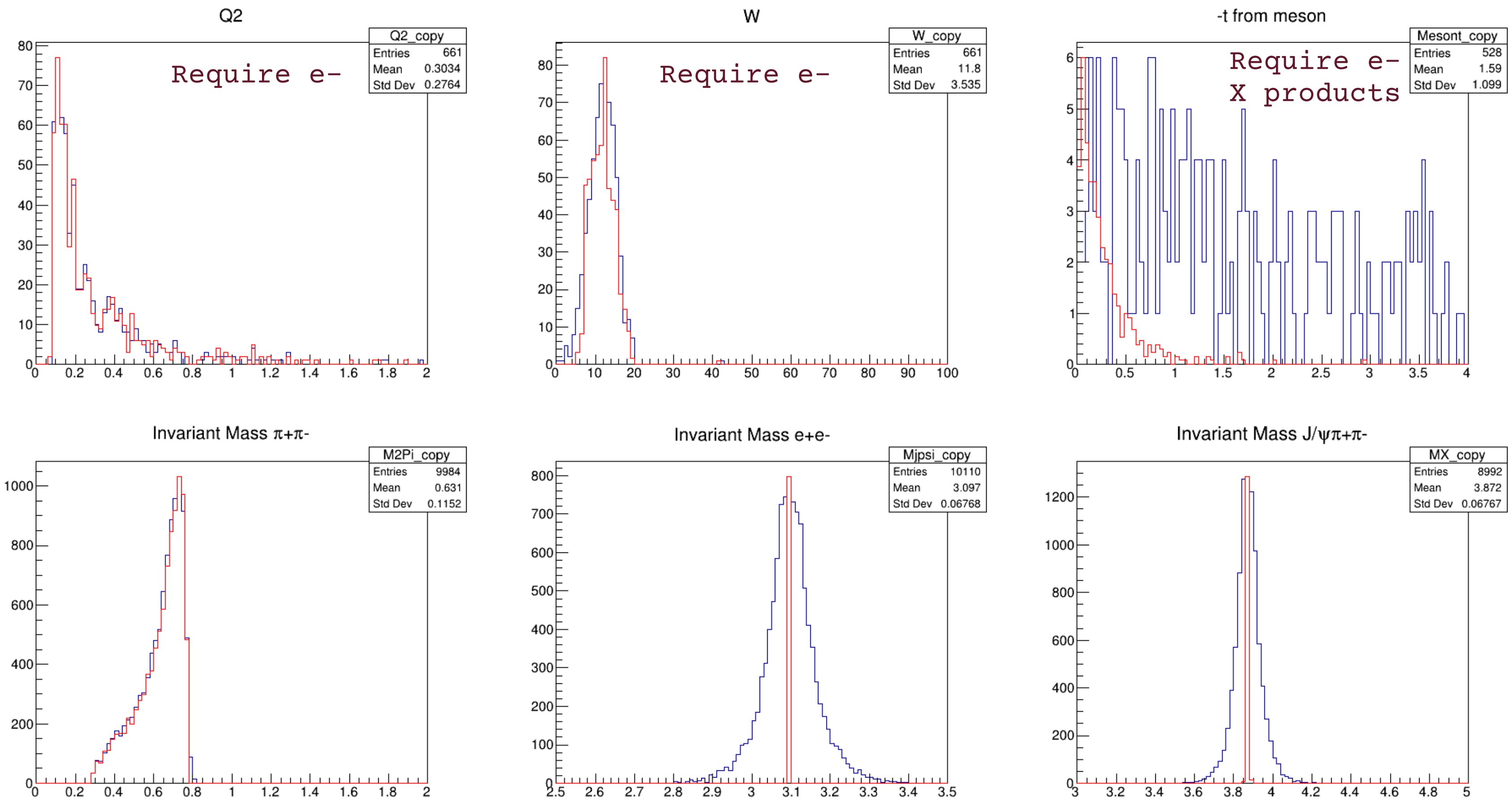

Generated
EIC-Smeared

Normalised to
Same max value

X decay product distributions

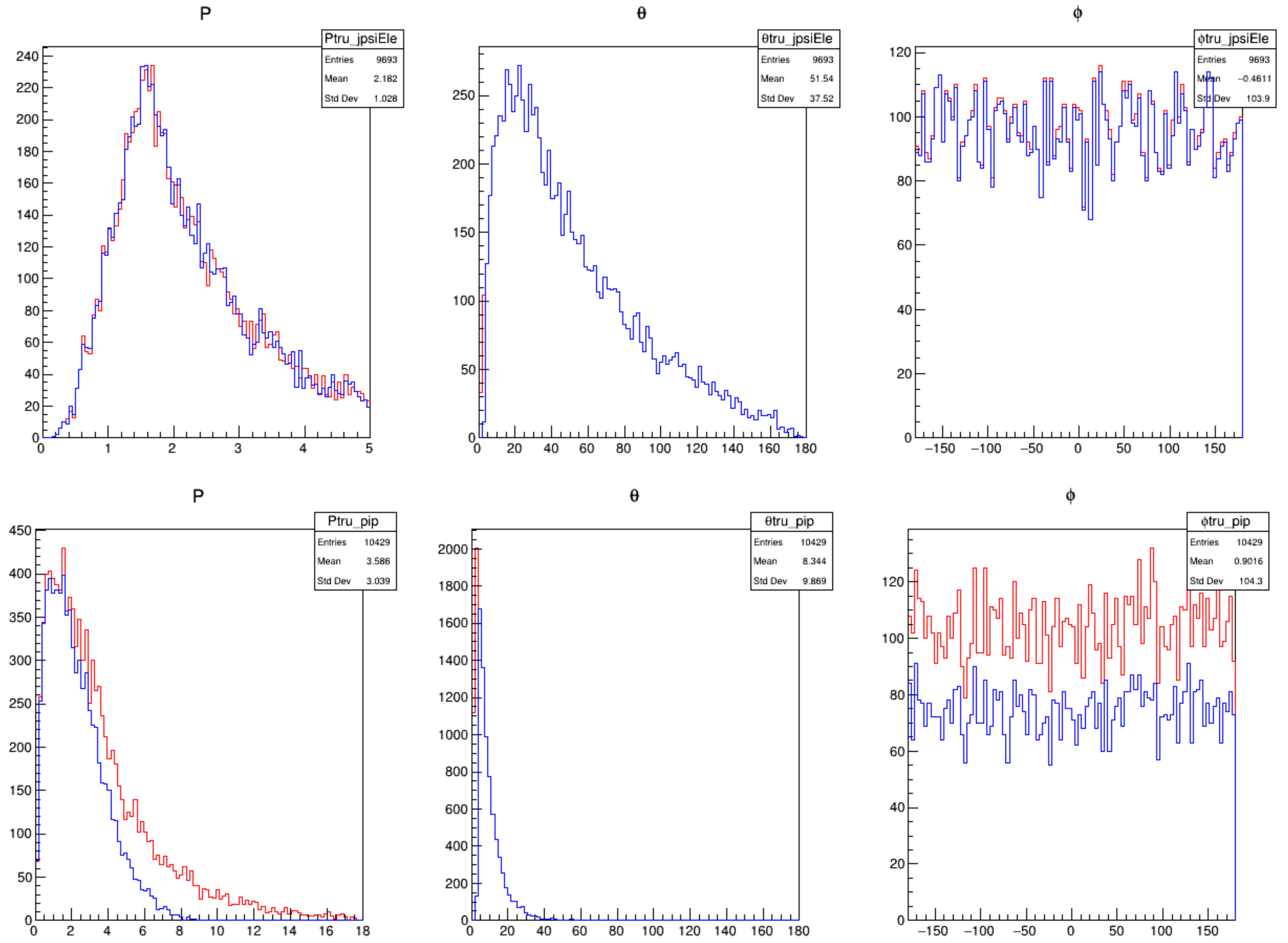

Jpsi e-

Generated

EIC-Smeared

5-41

high $E_{pr,}$ low W

Products → proton

18-275

Detector effects on Invariant Masses

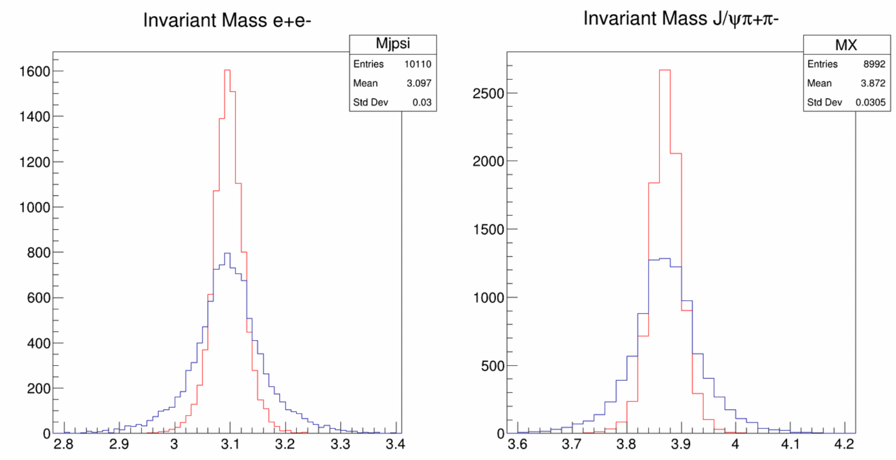

EIC smear for different field strengths
1.5T (65MeV)
3.0T (30MeV)
Typically 2x better
Resolution with 3T
**Note sure if the acceptance is
Correctly modelled for different fields

e/π seperation also significantly improves signal/background

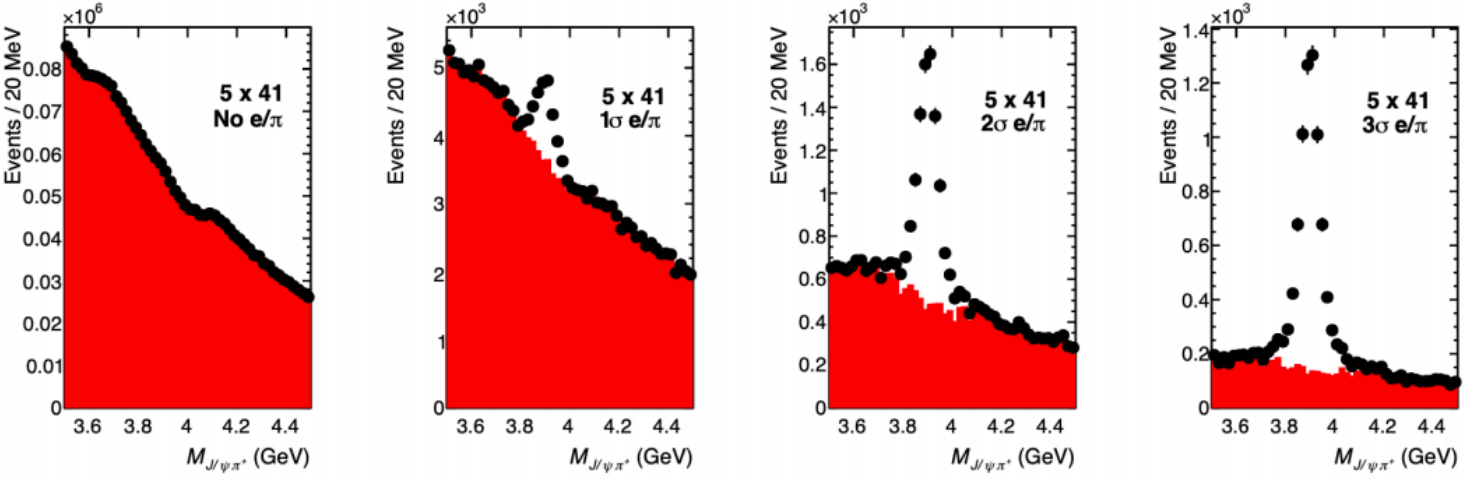

Pythia
$Z_c \rightarrow J/\psi\pi^+$

J.Stevens
from yellow report

X & Y & ψ(2S)

Invariant mass distributions for different beam/ magnetic fields

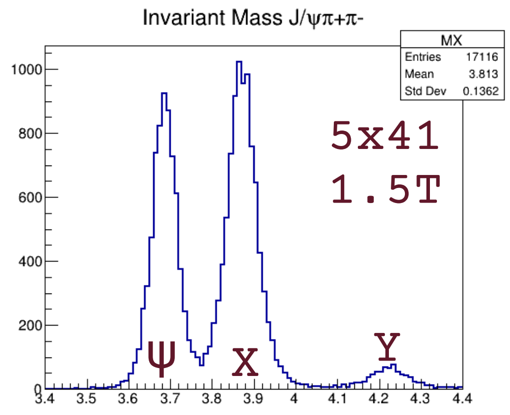

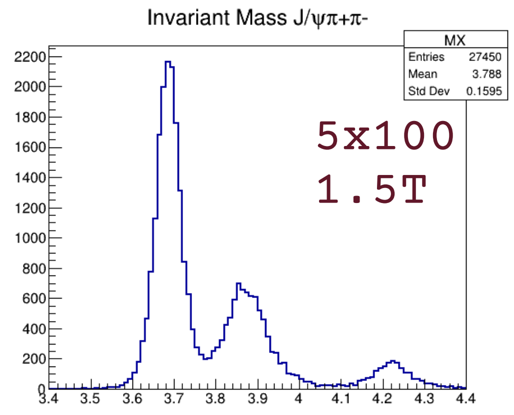

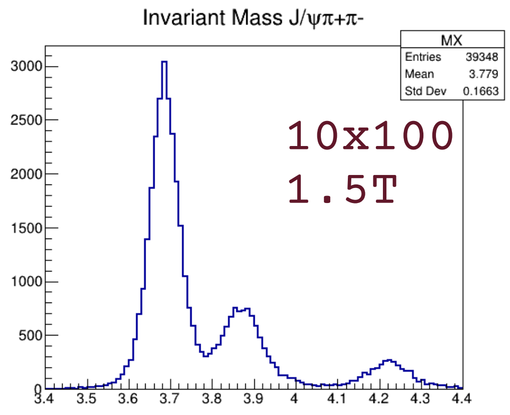

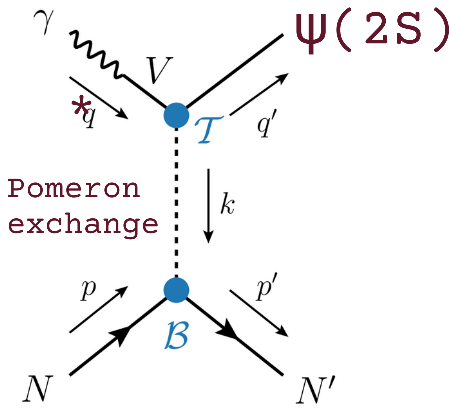

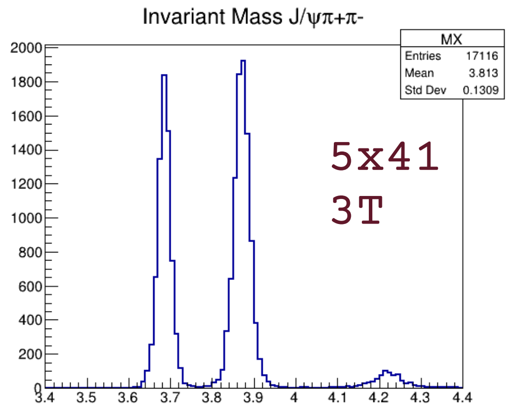

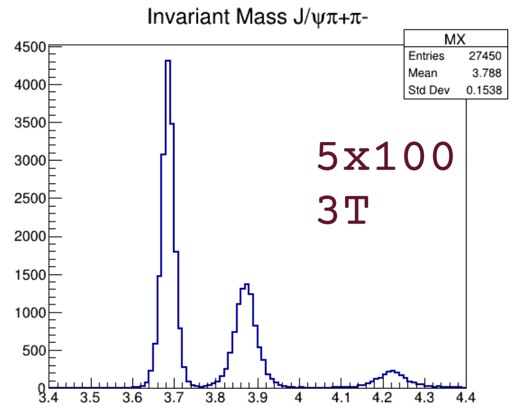

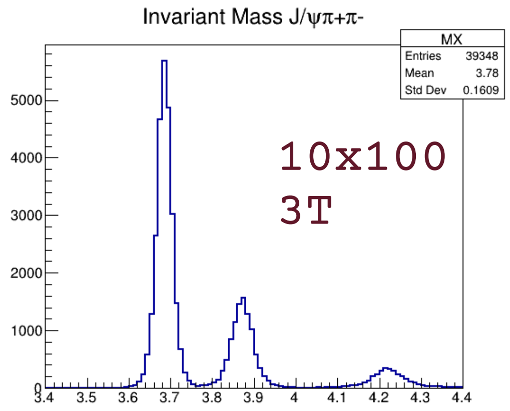

Decay angles

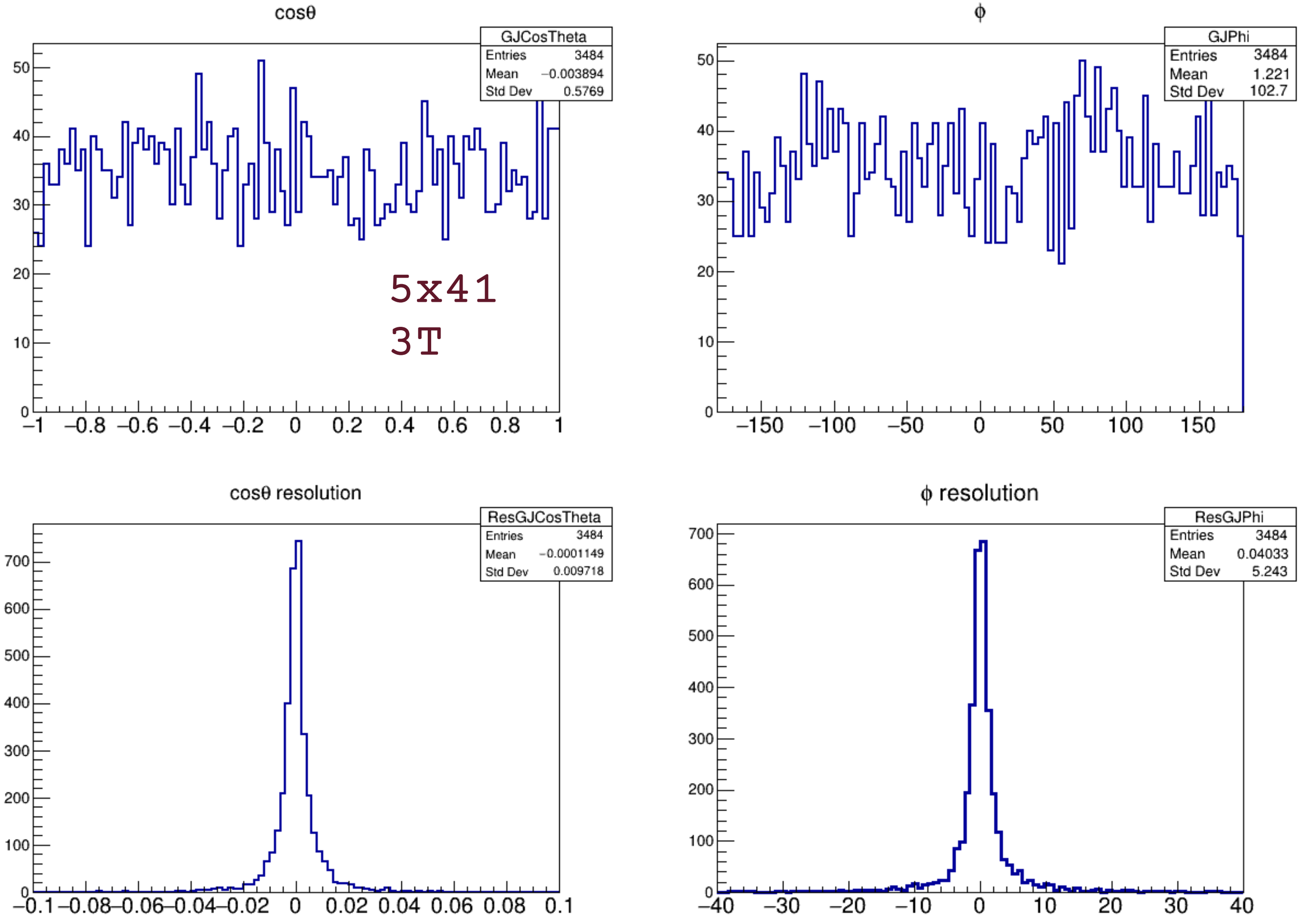

Decay angle of J/ψ in X rest frame

* Flat acceptances
* "Good" resolutions

  0.01 cosϑ

  5° Φ

  50% larger with 1.5T

* Should be good for Partial wave analysis etc.

Far Forward proton tagging

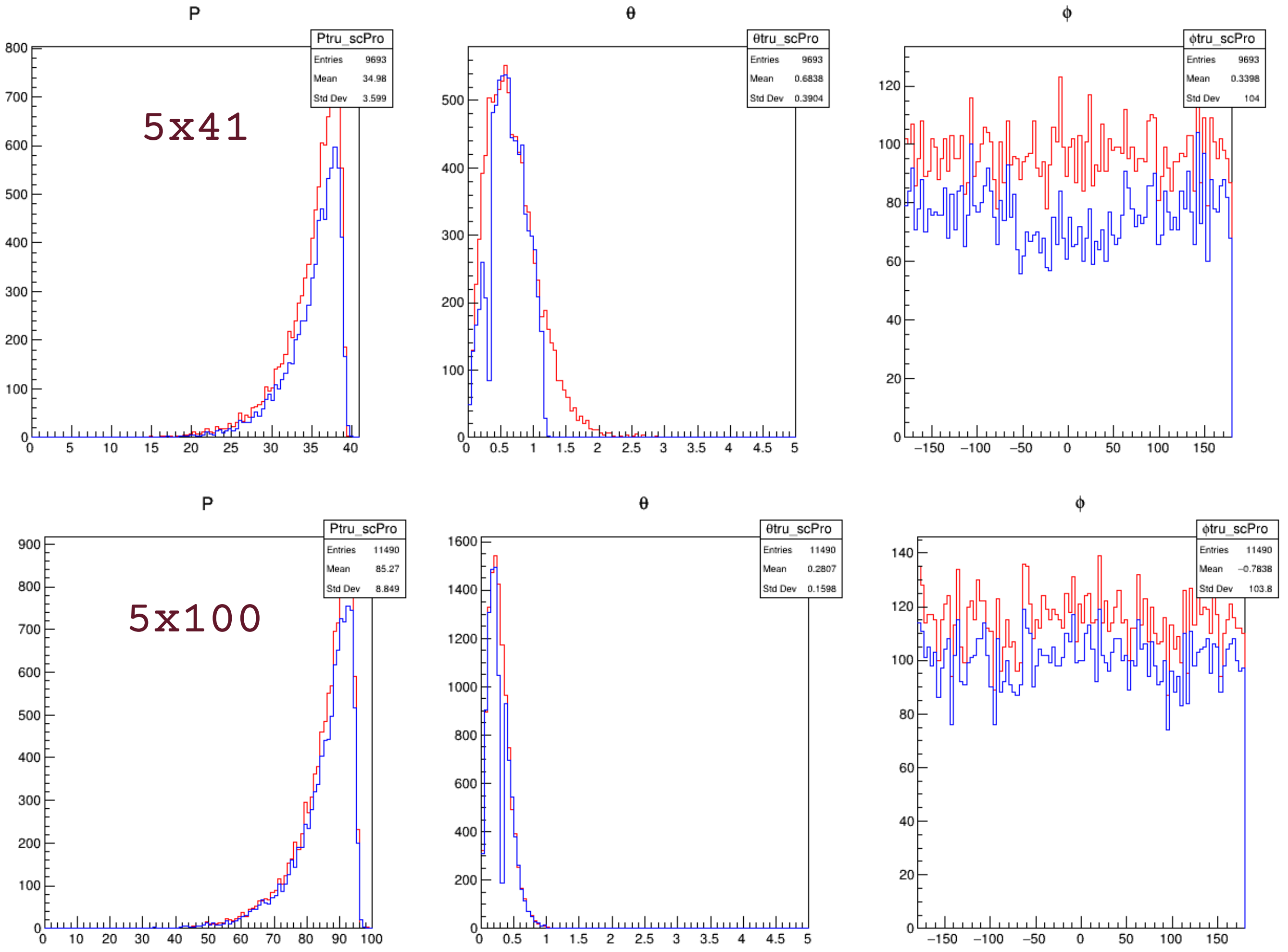

Determination of t

Another exclusivity constraint

Use EICsmear with FF

Planned far forward detectors offer good acceptance for XYZ production

Exclusivity variables

Calculate missing mass X from (e- + p - X)
Calculate missing transverse momentum from
(e- + p - X) and detected Far Forward proton
Red line => extra missing pion in final state

Missing mass does not offer great rejection
Missing transverse momentum much better, but requires detected proton

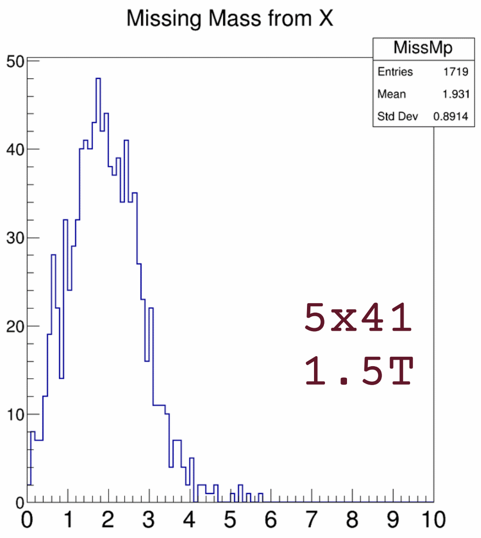

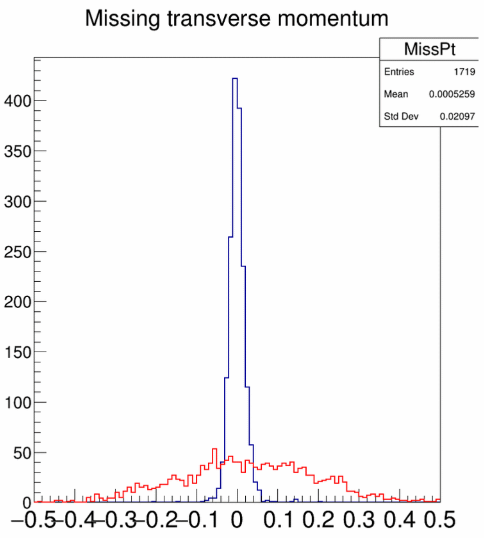

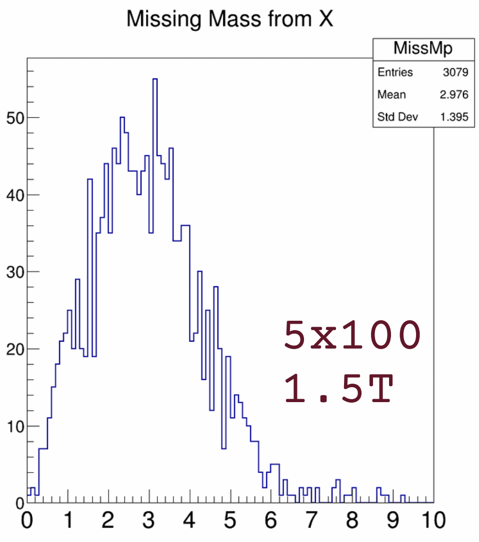

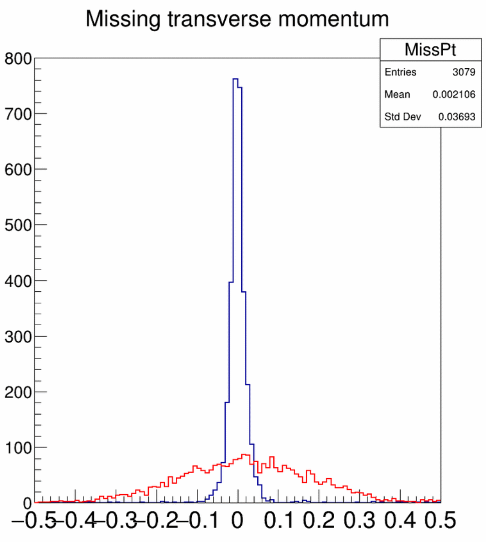

Summary

Event rates

- XYZ should be produced at the EIC with rates of 1-10k per week
- Reconstruction efficiency via decay products 50-100%
- 5 GeV e- and 100 GeV proton beam probably best configuration

Magnetic field

- 3T fields improves invariant mass resolution by factor 2
- Unclear trade-off in efficiency (low momentum threshold)

e- detection

- Allows determination of Q2, W, SpinDensityMatrix(decay angles)
- With nominal detector, efficiency 5-10%
- Low Q^2 tagger may significantly increase this

Proton detection

- Allows determination of t, exclusivity of final state
- Requires far forward detectors
- Current designs well matched to XYZ production

X